

CALIBRATING OPTICAL/IR INTERFEROMETRY VISIBILITY DATA

A.F. Boden¹

Abstract. By construction, optical (and near-infrared) interferometers typically have resolutions designed to resolve stellar and circumstellar features; such resolution is manifested as fringe contrast (or visibility) reduction for the resolved source. These same interferometers also experience visibility reductions due to instrumental and environmental limitations, so careful data calibration is required to accurately differentiate astrophysical and instrumental effects. This contribution discusses the basic techniques for and sources of errors in visibility data calibration, and selection strategies for sources used to calibrate the interferometer response.

1 Introduction – Calibrating Interferometer Visibility Data

An astronomical interferometer is a device that measures the interference (or attributes associated with the interference) of radiation from astronomical sources. Many astronomical applications use the interferometer to measure the amount of interference (or coherence) in the incident radiation field to obtain information about the source morphology on angular scales (or *spatial frequencies*) sampled by the interferometer. It is conventional to quantify this degree of coherence in the *interferometric visibility*; this visibility and how it related to astronomical source properties is discussed extensively in these proceedings by Hannif and others.

As an interferometer resolves an astronomical source (thereby obtaining useful information on its structure) the visibility (or fringe contrast) is reduced. The same interferometer also experiences visibility reductions due to instrumental and environmental limitations. To properly interpret visibility measurements we must assess the degree to which they are effected by limitations of the interferometer and its environment – in other words we need some methodology to differentiate astrophysical and instrumental effects in our data. In this way our interferometers are no different from any other measuring apparatus which imperfectly measures the *intrinsic* properties of our source. We typically describe the process of assessing and correcting for measurement imperfections

¹ Michelson Science Center, California Institute of Technology, Pasadena, CA

as *calibration* in general, and speak of *calibrating* data to represent the intrinsic source properties.

For the purposes of this discussion I will define this calibration as “the transformation of observables into a space where they have direct bearing on the (scientific) question at hand, and a critical evaluation of the precision (repeatability) and accuracy (correctness) of that transformation.” If the interferometer measures the coherence of our source radiation field, then our goal in calibration is to assess and correct for the *incoherence* of the interferometer and its environment.

Similar to other observational techniques, this degree of incoherence is typically estimated by quasi-contemporaneous measurement of *calibration sources* – astronomical sources that are used to derive a model of the interferometer response. The phenomenon that effect interferometer performance are many and varied, but in general are variable as a function of time, sky location, and brightness. Therefore, calibration sources are typically geometrically similar to the target (i.e. nearby in the sky) for both observational efficiency and instrumental and atmospheric variation reasons, and similar in apparent brightness to create a similar response by the interferometer.

In this discussion we will consider the process by which we calibrate visibility amplitude data on a science source. By common convention we will use visibility amplitude or just visibility to mean power-normalized visibility modulus, which is purely real, defined in the interval $[0,1]$, and 1 for an unresolved source measured by an ideal (i.e. perfectly coherent) interferometer. Operationally we typically measure visibility amplitudes (V_m) on one science target and one (or more) calibration source(s). We then transform these measured visibilities into “calibrated” visibility amplitudes (V_c) that represent an estimate of the *intrinsic* visibility (V_i , i.e. the response of the ideal interferometer) on our science target. Typically we assume a parametric form for the calibration transformation, and then estimate the transformation’s parameter values from measured visibilities and intrinsic properties of the calibration source(s).

2 Calibration Models and System Visibility

While the calibration transformations we consider can in theory have an arbitrary functional form, by far the most pervasive (and simple) form used for interferometer data calibration is a linear form:

$$V_c \propto V_m = CV_m$$

with the “constant” of proportionality C capturing the visibility reductions due to the incoherence of the interferometer. In this model C is independent of (in particular) V_m , so all measured visibilities are scaled by common factor, at least in a narrow, temporally and spatially local sense. Of course, applying this model to calibration source (calibrator) observations allows for an estimate of C :

$$C = V_{c-cal}/V_{m-cal}$$

Since V_{c-cal} represents the intrinsic visibility for the calibration source (V_{i-cal}), the apparent prescription for estimating C is to be able to *a priori* estimate V_{i-cal} . In the

special case where a calibrator source is *unresolved* at a given spatial frequency, the expected visibility (modulus) is 1, and C is:

$$C = V_{i-cal}/V_{m-cal} \rightarrow 1/V_{m-cal} \equiv 1/V_{sys}$$

where we have introduced the *system visibility* or point-source response V_{sys} of the interferometer, the expected visibility for an ideal point source as measured by a real (imperfect) interferometer. The system visibility is sometimes known by other names: point-source response, visibility transfer function, or interferometric efficiency factor. So the standard form of our linear calibration model for the science target is:

$$V_{c-trg} = (1/V_{sys})V_{m-trg} \quad (2.1)$$

with

$$V_{sys} = V_{m-cal}/V_{i-cal} \quad (2.2)$$

Equation 2.2 gives a the form of the system visibility for a general (i.e. possibly resolved) calibration source.

Following our calibration definition from §1, we must assess the uncertainty (variance) in our calibration calculation, which takes the form:

$$\begin{aligned} \sigma_{V-c-trg}^2 &= (1/V_{sys})^2 \sigma_{V-m-trg}^2 + (V_{m-trg}/V_{sys}^2)^2 \sigma_{V-sys}^2 \\ &\approx V_{sys}^{-2} [\sigma_{V-m-trg}^2 + (V_{m-trg}V_{m-cal})^2 (\sigma_{V-m-cal}^2 + V_{sys}^2 \sigma_{V-i-cal}^2)] \end{aligned} \quad (2.3)$$

where $\sigma_{V-m-trg}$ and $\sigma_{V-m-cal}$ represent visibility measurement uncertainties for the target and calibration source respectively, and $\sigma_{V-i-cal}$ represents the uncertainty in the *a priori* prediction of the calibrator intrinsic visibility. In the limit that the target and calibrator visibilities are measured well, the limiting calibration error becomes the ability to predict the calibrator intrinsic visibility.

More complicated calibration models are possible and are beyond the scope of this contribution. Interested readers are referred to Mozurkewich et al. 1991 and Boden et al. 1998.

3 Choosing Calibration Sources

To this point the discussion is independent of the calibrator's fundamental nature. However Eq. 2.3 frames many of the practical issues of choosing calibrators. The term in $\sigma_{V-m-cal}$ represents the calibrator visibility measurement uncertainty. This error is usually strongly correlated with the source brightness. Minimizing the contribution from this term implies a calibrator should be bright enough that its fringes can be well-measured by the interferometer. A common practice is to choose calibrators of similar brightness to the science target, then $\sigma_{V-m-trg}$ and $\sigma_{V-m-cal}$ often contribute similarly in Eq. 2.3. More extensive discussion of fringe measurement is given in citeColavita1999.

However the term in $\sigma_{V-i-cal}$ is different from the measurement error; it goes to the source astrophysical properties in general, and captures the uncertainty in *a priori* predicting the calibrator's intrinsic visibility in particular. In theory an arbitrary source can serve as a calibrator, but the desire to accurately predict intrinsic visibilities means in

practice only simple sources have been used for such purposes. The simplest sources for our purposes are *effectively single* stars: stars that either have no luminous companion, or no luminous companion that can be detected by the interferometer as it measures fringes of the primary.

Predicting a single calibrator’s intrinsic visibility V_{i-cal} requires assuming a morphological model. Again, the common practice is to assume the simplest practical model – that of a luminous uniform disk against a dark background. The predicted visibility amplitude from a uniform disk of apparent diameter Θ_{cal} is given by:

$$V_i = \frac{2J_1(\pi\Theta B_\perp/\lambda)}{\pi\Theta B_\perp/\lambda} \quad (3.1)$$

with J_1 is the first-order Bessel function, B_\perp is the interferometer baseline length perpendicular to the star direction, and λ is the interferometer operating wavelength (see Boden 1999 or Hannif in these proceedings for a derivation). Fig. 1 depicts this disk visibility and its first derivative as a function of Θ_{cal} . This visibility model exhibits the expected behavior: $V_{i-cal} \sim 1$ for an unresolved source (i.e. $\Theta_{cal} \ll \lambda/B$), and $V_{i-cal} \ll 1$ for a resolved source (i.e. $\Theta_{cal} \sim \lambda/B$).

To use Eq. 3.1 one must have a working estimate of Θ_{cal} . We will consider techniques for estimating Θ_{cal} in § 4, but for the moment it suffices to observe that any working angular diameter estimate will be of finite precision with uncertainty $\sigma_{\Theta-cal}$. This model allows an estimate the calibration error contribution in Eq. 2.3 from finite calibrator diameter error:

$$\sigma_{V-i-cal} \approx \left| \frac{dV}{d\Theta_{cal}} \right| \sigma_{\Theta-cal} \quad (3.2)$$

The calibration error contribution from $\sigma_{V-i-cal}$ in Eq. 2.3 can be minimized either by minimizing the fundamental uncertainty in the model diameter ($\sigma_{\Theta-cal}$, i.e. knowing the calibrator diameter well), or better, by minimizing the sensitivity of the calibration on the calibrator model diameter error – i.e. minimizing $|dV_{i-cal}/d\Theta|$. As seen in Fig. 1, $|dV_{i-cal}/d\Theta| \rightarrow 0$ in the unresolved limit ($\Theta \ll \lambda/B_\perp$), so we are motivated to work with calibrators that are as unresolved as practical.

From this discussion we conclude that a good calibrator must be bright enough that its fringe parameters can be well-measured. Further, we want these calibrators to be as unresolved (i.e. apparently small) as possible so as to minimize the calibration error due to calibrator modeling error. It will turn out that these two objectives are fundamentally at odds with each other. These considerations lead us to the practical necessity of *estimating* angular diameters in the evaluation of potential calibrators.

4 Indirectly Estimating Stellar Angular Diameters

As argued above, we are motivated to consider stars that are unresolved by the interferometer ($\Theta \ll \lambda/B_\perp$). To get a sense of scale involved consider first our own sun (physical diameter ≈ 0.01 AU) as viewed from a typical solar neighborhood distance of 10 pc – its apparent diameter would be on the order of 1 milliarcsecond (10^{-3} arcseconds, mas). This quick assessment was possible because we have have an accurate measurement of the sun’s physical radius, and we assumed a definite distance in this example; in

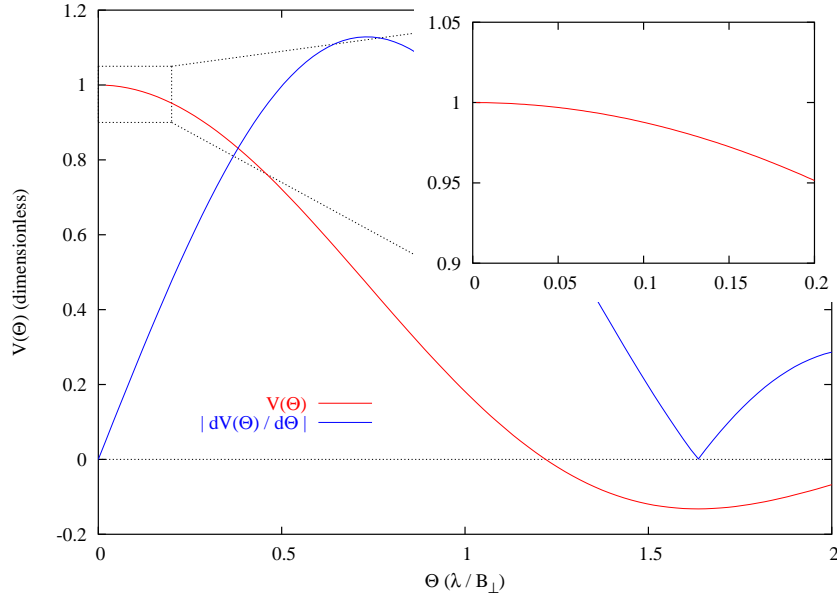


Fig. 1. Disk Visibility and Derivative. The predicted visibility V of a uniform disk as a function of its apparent diameter Θ (Eq. 3.1) and the first derivative $|dV/d\Theta|$ are given. Θ_{cal} is in units of the projected interferometer fringe spacing λ/B_{\perp} . Inset is a closeup of the unresolved limit ($\Theta \ll \lambda/B_{\perp}$) where $V \rightarrow 1$ and $|dV/d\Theta| \rightarrow 0$. Calibration sources are typically chosen to be as unresolved as possible so as to minimize systematic calibration error from finite knowledge of Θ_{cal} and large values of $|dV/d\Theta|$.

the general case we lack at least one of these quantities for most other stars in the sky. So our estimates of apparent diameter will necessarily appeal to more indirect methods.

While many techniques exist for such indirect estimates, the most broadly applicable and prevalent techniques are based on the definition of a star's *effective temperature* (Binney & Merrifield 1998, Cox et al. 1999):

The effective temperature of a star is the temperature of a black body with the same emittance (luminosity per surface area, f_{Bol}) as the star and is defined according to the Stefan-Boltzmann law ($f_{Bol} = \sigma T_{eff}^4$).

The effective temperature is not a thermodynamic temperature at all, instead it is defined by (and serves as proxy for) a star's specific radiant emittance or surface brightness. With this definition we can consider a star of physical radius R ; evidently the star's total luminosity is given by its radiant emittance times its surface area:

$$\mathcal{L} = 4\pi R^2 \sigma T_{eff}^4$$

Viewed at a distance D the incident bolometric flux (total radiant flux per unit collecting

area) is

$$\mathcal{F}_{Bol} = \mathcal{L}/4\pi D^2 = (R/D)^2 \sigma T_{eff}^4 = (\Theta/2)^2 \sigma T_{eff}^4$$

having identified the apparent diameter $\Theta = 2R/D$ in the last equality. The stars apparent diameter is then just:

$$\Theta = \sqrt{\frac{4F_{bol}}{\sigma T_{eff}^4}} \approx 8.17 mas \times 10^{-0.2*(V+BC)} [T_{eff}/5800K]^{-2} \quad (4.1)$$

with the second approximation capturing the star's bolometric flux in terms of its apparent (Johnson) visual magnitude V and the bolometric correction BC appropriate for its spectral type.

Eq. 4.1 is deceptively simple: it seems all we need for an operational angular diameter estimate is to measure a star's bolometric flux and effective temperature. This is true, but it leaves open the question of exactly how well one can estimate bolometric flux and effective temperature. Operationally these quantities are most securely estimated through spectral energy distribution modeling: constructing a model of the spectral energy distribution for the source, integrating it to estimate the bolometric flux, and combining that with (some) estimate of the effective temperature to compute the apparent diameter estimate through Eq. 4.1. An example of this kind of SED analysis is given in Fig 2, where we have estimated the apparent diameter of the *effectively* single star 51 Peg (HD 217014; Mayor & Queloz 1995, Marcy et al 1997) by various SED modeling techniques. Cohen et al 1999 and Merand et al 2005 have published studies of angular diameters estimated by SED modeling techniques; the interested reader is referred there for more extensive discussions.

Related techniques are employed in the Infrared Flux Method (IRFM) used by Blackwell and collaborators (e.g. Blackwell & Lynas-Gray 1994 and references therein), and Mozurkewich et al. 1991, van Belle et al 1999, and Kervella et al 2004 have used color indices (e.g. $V - K$) as proxies for effective temperature estimates. In the author's opinion these methods are less reliable than more comprehensive SED modeling, but offer accessible alternatives for quick estimation.

It is important to keep in mind that indirect diameter estimation eventually involves the source effective temperature estimate. Using even a high-fidelity SED template for photometric (e.g. Fig. 2) or spectroscopic modeling, the resulting diameter estimate is no more *accurate* than the effective temperature calibration of the template. For this reason it is important to have a healthy skepticism for estimated angular diameters, and a keen eye on how likely diameter errors can couple into systematic errors in the calibrated data set through Eqs. 2.3 and 3.2.

Finally it is noteworthy that the apparent brightness and apparent size of a star are inextricably connected; this is exhibited in Eq. 4.1, which shows how the apparent size of a star decreases as the apparent magnitude (Johnson V) increases (i.e. the source appears dimmer – in the limit of constant T_{eff} and BC). In § 3 we argued that calibrators should be both apparently bright (for favorable SNR in measuring fringe parameters) and apparently small (for favorable control of calibration errors through Eq. 3.2). Eq. 4.1 makes it clear that these two objectives are fundamentally at odds with each other. Cal-

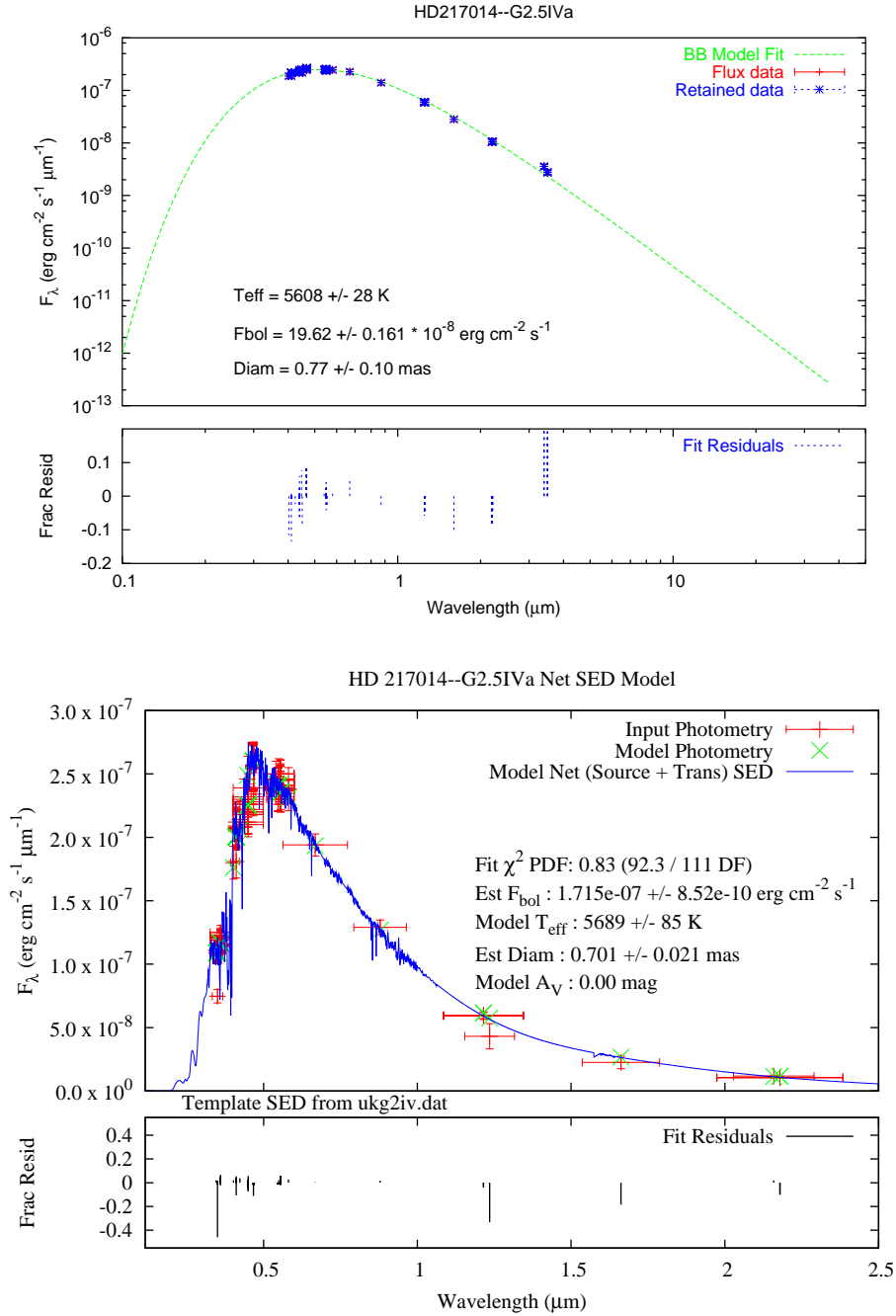


Fig. 2. Modeling of the spectral energy distribution for 51 Pegasi (HD 217014). Top: the SED template is a single-temperature Plank black body photosphere model. The agreement between data and model is reasonably good, leading to a reasonable estimate of source apparent diameter (0.77 ± 0.10 mas). Bottom: the SED of the same source as modeled using a high-fidelity SED template from Pickles 1998. A similar angular diameter results from this computation (0.70 ± 0.02 mas).

ibrator selection calls for striking a balance between brightness and calibration accuracy; Merand et al 2005 discuss quantitative methods for striking this balance.

5 Stellar Multiplicity

Binary stars are prevalent among stars in the solar neighborhood. In the definitive study for solar-like stars Duquennoy & Mayor (1991, DM91) determined that roughly 1/2 of all solar-type primary stars had stellar companions, and similar statistics are thought to hold for other stellar types. From the standpoint of identifying potential visibility calibrators the prevailing wisdom is multiplicity is to be avoided. Surely this is an overstatement; simple visual binaries with separations of a few arcseconds or more pose no significant risk in application as calibrators (hence our use of the term effectively single in § 3). However, multiplicity over angular scales that would effect visibility measurements *should* be avoided – the modeling of visibilities from binary calibrators (e.g. $\sigma_{V-i-cal}$ in Eq. 2.3) excessively complicates the calibration process. Figure 3 depicts the observed DM91 binary period distribution (corrected for detection efficiency), and the log-normal analytical distribution model provided by DM91. For the purposes of the present discussion I have added a calculation of the implied angular semi-major axis assuming a typical system mass of $1.6 M_{\odot}$ and system distance of 25 pc. If we were to exclude systems with projected separations of $5''$ (the dotted vertical line in Fig. 3) or less we would exclude approximately 60% of the observed DM91 population.

The operational question is how to identify multiple systems in the experiment planning phase. Here there are no great pearls of wisdom beyond detective work. Some of the standard sources for the identification of binarity are: the SIMBAD stellar database hosted by Centre de Données astronomiques de Strasbourg¹, various spectroscopic binary catalogs such as that by Batten² (1989), the Washington Double Star catalog³, and the Hipparcos astrometric catalog – in particular the orbital and component solution annexes⁴ (ESA 1997).

Even having performed due diligence to screen against *known* multiplicity, detections of previously unknown multiplicity sometimes occur at the telescope. This is particularly true for large-aperture interferometers such as the VLTI (see Scholler in these proceedings) and the Keck Interferometer (KI, Colavita et al 2003), where the high sensitivity brings fainter and more poorly understood sources accessible. Contingency planning for calibrators being detected as binary is advisable if one is using previously unvetted calibrators.

6 Experiment Planning Tools

The preceding discussion has left open the question of how to incorporate these various considerations in the planning of an actual experiment. Fortunately, there are several

¹see <http://cdsweb.u-strasbg.fr/>

²available at <http://vizier.u-strasbg.fr/cgi-bin/VizieR>

³available at <http://ad.usno.navy.mil/wds/>

⁴available at <http://astro.estec.esa.nl/Hipparcos/>

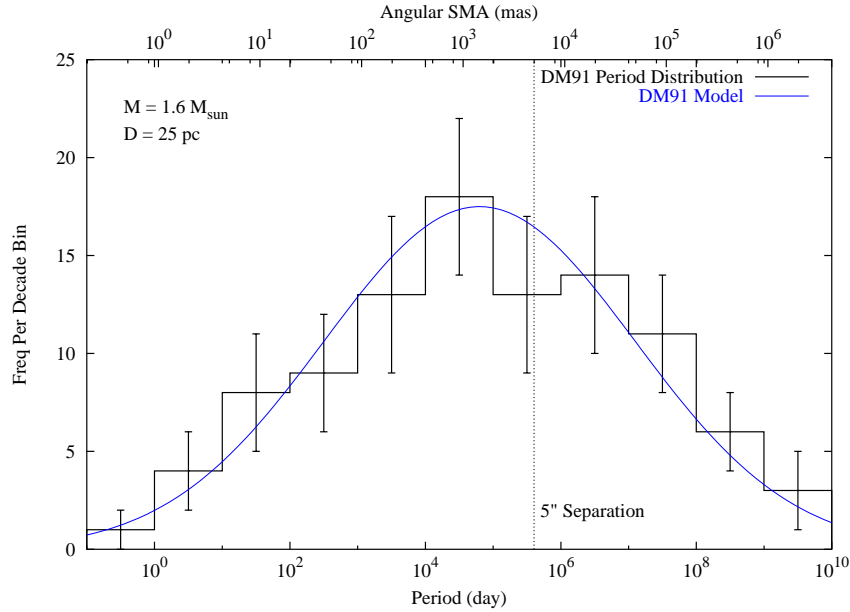


Fig. 3. Observed Period Distribution For Solar-Like Binary Stars (from Duquennoy & Mayor 1991). On the top horizontal axis we indicate the implied angular semi-major axis assuming a system mass of $1.6 M_{\odot}$ and a distance of 25 pc. A dotted vertical line is given at $5''$ (see text discussion).

software suites available to assist users in incorporating these considerations in the design of interferometer experiments. The ASPRO package from JMMC (Jean Marie Mariotti Center; http://www.mariotti.fr/aspro_page.htm), the getCal package from MSC (Michelson Science Center; <http://msc.caltech.edu/software/getCal>), and the SearchCal package (associated with ASPRO; Bonneau et al 2006), and the VLTI Visibility Calculator and Calibrator Selection tools from ESO (European Southern Observatory, both available from <http://www.eso.org/observing/etc>) all integrate various threads from the prior discussion to facilitate the user establishing a plan for an optical interferometry experiment. As observing details will vary with different instruments and observing modes, we recommend the reader consult documentation and support resources specific to their target instrument.

7 Observing and Calibrating Visibilities

Once potential calibrators are identified for a particular experiment, it is then necessary to define the parameters for the observing, typically addressing such issues as the number of calibrators to be carried in the experiment, the relative ratio of calibration to science observations, and any specific order for the observations to proceed in. With regard to the

number, a conventional rule of thumb is two calibrators carried through the experiment duration is a safe strategy. This allows extensive cross-checking between calibrators for consistency, and some redundancy in the event that one of the selected objects exhibit unexpected and/or unwanted features in the data. With regard to the ratio of science and calibration data, assuming that the instrument performs similarly on the target and calibrators, the optimal (i.e. minimum-variance on the calibrated observation SNR) ratio of target to calibrator data is 1:1. However, external operational objectives such as overall instrument science throughput may well override the desire to optimize the SNR on individual observations.

It is our experience at PTI and KI that the overall best calibration performance results when target and calibration measurements are interleaved in short (e.g. < 15 min) cycle times – this amounts to the visibility analog of “chopping” between target and calibrator. These chop cycles allow the calibration model to be responsive to temporal variations in the instrument or environment (e.g. see Boden et al. 1998). Similarly the choice of calibrators near the target both serve to make the chop cycles more efficient and mitigate the effects of any sky position-dependent effects in either the instrument or atmosphere.

Finally it is important to keep in mind the calibration limitations imposed by finite error in the calibrator diameter (e.g. Eq. 3.2); calibration precision is not the same thing as accuracy. Recent work by van Belle & van Belle (2005) discuss this point in some detail.

8 Summary

In this contribution I have introduced the basic concepts for calibrating interferometric visibility data. The detailed implementation of strategies for evaluating calibrators and preparing experiment plans are best discussed in the context of specific instruments and observing modes. Many of the basic considerations that facilitate well-calibrated interferometry experiments can be implemented in the context of observation planning software such as the ASPRO and getCal packages, both referenced above.

I have dealt mainly with issues of the astrophysics of potential calibration sources (e.g. the modeling of calibrator SEDs, the frequency and identification of multiplicity). However there are potentially other instrument-specific factors that should be considered in selecting calibration sources. For instance, for big-aperture interferometers such as VLTI and KI, the Adaptive Optics correction performance will be a function of brightness, and may be a function of color. So it may become necessary to approximately match brightnesses and colors between target and calibrators. Another possible consideration is in the delay coverage of the interferometer for targets at the extremes of declination coverage where small differences in sky position can result in surprisingly large differences in temporal accessibility.

References

- Akeson, R.L. et al. 2000, ApJ 543, 313.
- Batten, A.H. et al. 1989, PDAO 17 1.

- Blackwell, D., and Lynas-Gray, A. 1994, *A&A* 282, 899.
- Binney, J. & Merrifield, M. 1998, "Galactic Astronomy", Princeton University Press.
- Boden, A.F. et al. 1998, *Proc. SPIE* 3350, 872.
- Boden, A.F. 1999, "Elementary Theory of Interferometry", *Proc. 1999 Michelson Summer School*, (<http://sim.jpl.nasa.gov/michelson/iss1999/index.html>).
- Bonneau, D. et al 2006, *astro-ph/0607026*.
- Bord, P. et al 2002, *A&A* 393, 183.
- Cohen, et al 1999, *AJ* 117, 1864.
- Colavita, M. et al 2003, *ApJ* 592, L83.
- Cox, A.N. et al. 1999, *Allen's Astrophysical Quantities*, AIP Press.
- Duquennoy, A., and Mayor, M. 1991, *A&A* 248, 485.
- ESA 1997, *The Hipparcos and Tycho Catalogues*, ESA SP-1200.
- Ghez, A.M. et al. 1991, *AJ* 102, 2066.
- Kervella, P. et al 2004, *A&A* 426, 297.
- Koresko, C.D. 2000, *ApJ* 531, L147.
- Marcy, G.W. et al. 1997, *ApJ* 481, 926.
- Mayor, M. and Queloz, D. 1995, *Nat* 378, 355.
- Merand, A. et al 2005, *A&A* 433, 1155.
- Mozurkewich, D. et al. 1991, *AJ* 101, 2207.
- Pickles, A. 1998, *PASP* 110, 863.
- Rybicki, G.B. and Lightman, A.P. 1979, *Radiative Processes in Astrophysics*, John Wiley & Sons.
- van Belle, G. et al 1999, *AJ* 117, 521.
- van Belle, G. & van Belle, G. 2005, *PASP* 117, 1263.